Decoherence and Thermalization at Finite Temperatures for Quantum Systems

Mark A. Novotny[1], Fenping Jin[2], Shengjun Yuan[3], Seiji Miyashita[4], Hans De Raedt[5], and Kristel Michielsen[2,6]

[1] Mississippi State University, [2] Jülich Supercomputing Centre, [3] Radboud University, [4] University of Tokyo, [5] University of Groningen, [6] RWTH Aachen University

Introduction and Motivation

We study a general closed quantum entirety, considered to be a subsystem with Hamiltonian H_S, an environment or bath with Hamiltonian H_E, and a Hamiltonian with overall strength λ which couples S and E. The entirety $S+E$ evolves via the time-dependent Schrödinger equation with Hamiltonian $H=H_0+\lambda H_{SB}=H_S+H_E+\lambda H_{SB}$. The dimension of the entirety *is* $D=D_S D_E$. We assume that the entirety is in the canonical-thermal-state ensemble at inverse temperature $\beta=1/T$ (with $k_B=\hbar=1$).

Methods

The reduced density matrix for S is $\tilde{\varrho}_S = Tr_E\, \varrho$, with elements given by Eq.(1). Our measure of decoherence $\sigma(t)$ is given by a function of the off-diagonal elements of $\tilde{\varrho}_S$ (in the basis where H_S is diagonal) as in Eq.(2), while our measure of thermalization $\delta(t)$ is given by a function of the diagonal elements as in Eq.(3). In Eq.(3) $b(t)$ is a fitting parameter, and the superscripts on the energies stand for S or E.

The state $|\Psi_0\rangle$, given by Eq.(5), is a random infinite-temperature ($\beta=0$) state of the entirety $S+E$. The coefficients $d_{i,p}$ are complex Gaussian random numbers, and the normalization is given by Eq.(6). The canonical-thermal state is given by Eq.(7), and is a normalized pure state at a finite temperature, $T=1/\beta$. All such states $|\Psi_\beta\rangle$ form the canonical-thermal-state ensemble.

The free energies for the entirety, S, and E are, respectively, $F(\beta)$, $F_S(\beta)$, and $F_E(\beta)$; ground-state degeneracies are g, g_S, g_E.

Perturbation Results

We have performed perturbation theory calculations for a general entirety, for small λ. The calculations use Eq.(4), and are performed over the entire canonical-thermal-state ensemble. The lowest order term has $\lambda H_{SE}=0$, an uncoupled but entangled entirety. After lengthy calculations, general expressions at long times for σ are obtained, Eq.(8), to be a function of the free energies at particular temperatures. The limit for σ for infinite temperature is in Eq.(9), and for very low temperatures in Eq.(10). A similar expression for the thermalization is presented as Eq.(11).

Computational Results

We have performed large-scale calculations with a ring of spin ½ particles, with the number of such particles $N=N_S+N_E$. Random interactions are chosen for H_E ($\Omega_{ij}\in[-4/3,4/3]$) and H_{SE} ($\Delta_{ij}\in[-4/3,4/3]$), and ferro- or antiferromagnetic ($|J|=1$) for H_S. Relaxation in time is shown in Fig.1, and time-or-disorder averages in Fig.2. Dependences on different N_E, N_S, λ, and β are shown in Figs.3-5. Comparisons with no adjustable parameters to Eq.(8) are in Figs.6,7, note different g_S values.

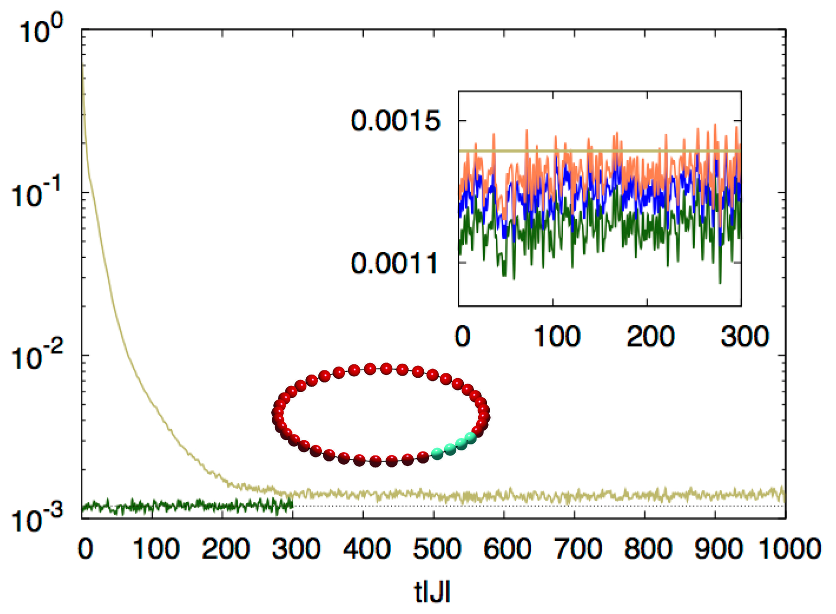

Fig. 1. $N_S=4$, $N_E=22$, $\beta|J|=0.9$, $\lambda=1$ with initial states of ***UDUDY*** or ***X***, with ***X*** and ***Y*** states from the appropriate canonical-thermal-state ensemble.

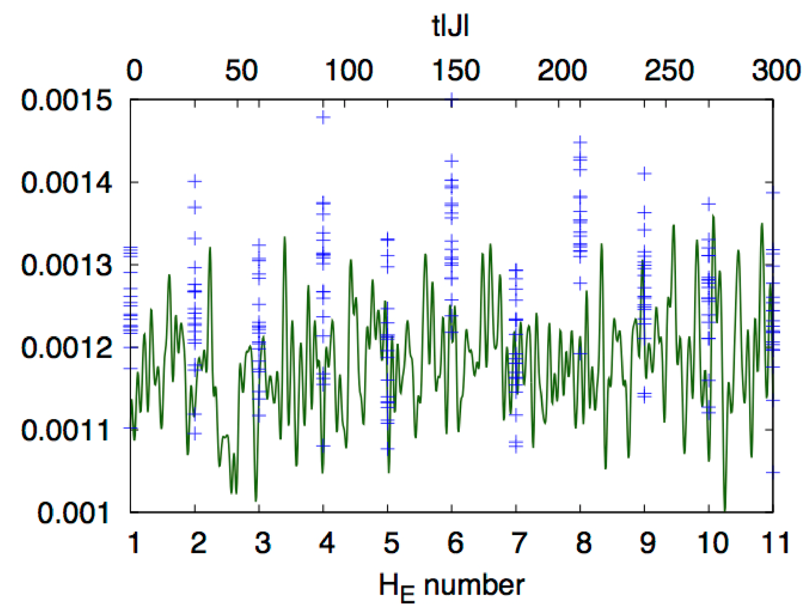

Fig. 2. $N_S=4$, $N_E=22$, $\beta|J|=0.9$, $\lambda=1$ with an initial state ***X***, showing results of averaging over time, H_E, and initial states from ***X***.

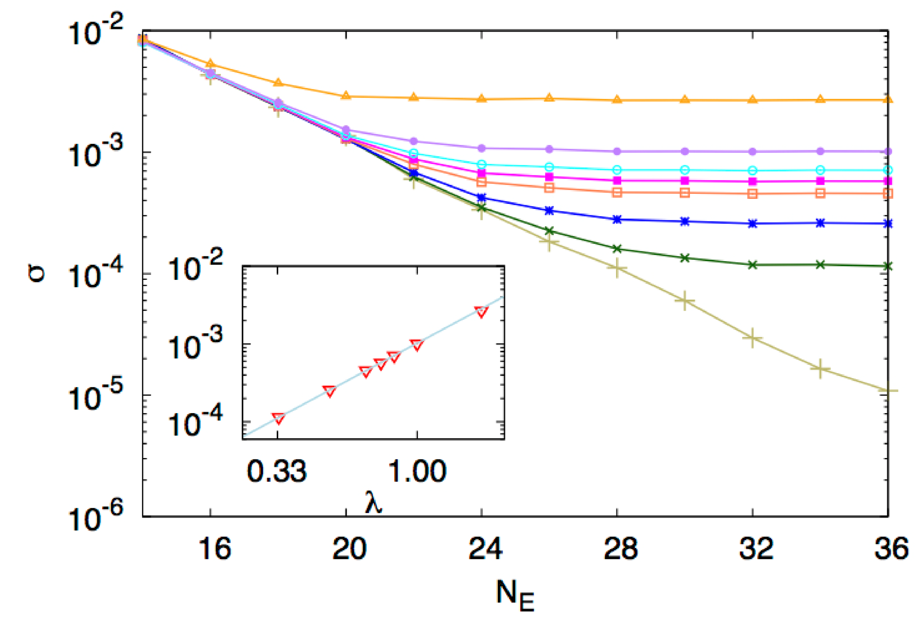

Fig. 3. $N_S=4$, $\beta|J|=0.9$, with different values of N_E and λ. Inset has $N_E=36$ results.

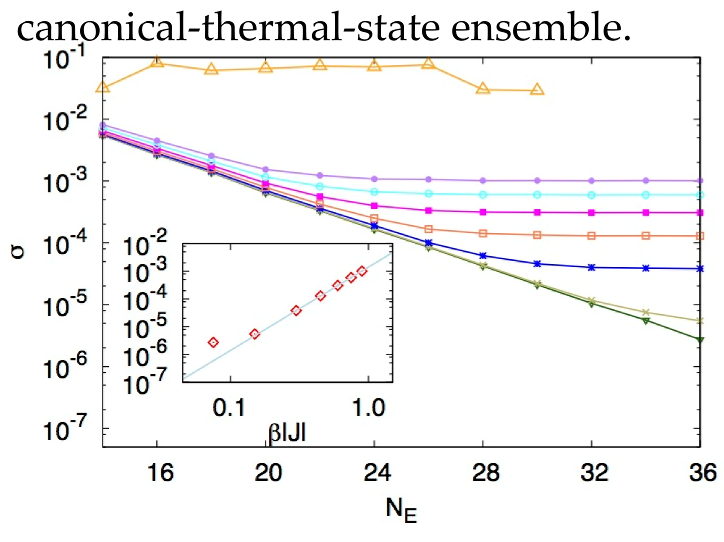

Fig. 4. $N_S=4$, $\lambda=1$ for different values for $\beta|J|$ and N_E. Inset are $N_E=36$ results.

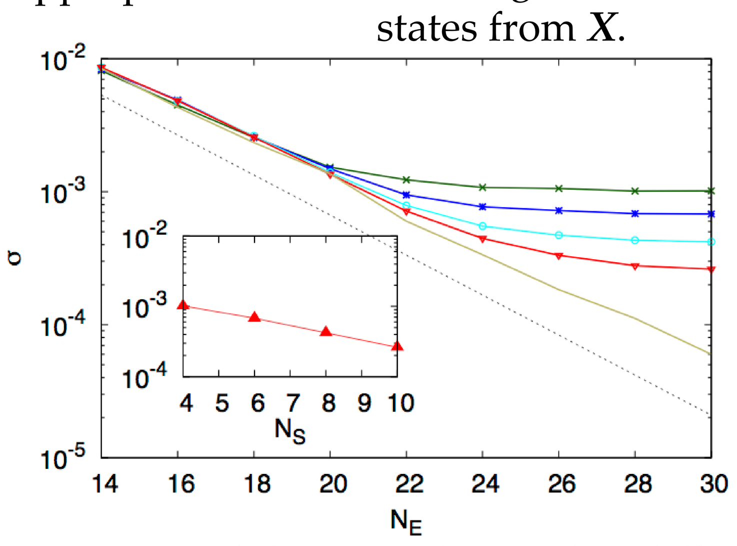

Fig. 5. $\beta|J|=0.9$ and $\lambda=1$ for different values for N_S and N_E. The dark khaki line is for $\lambda=0$. Inset are $N_E=30$ results.

Equations

$$\widetilde{\rho}_{ij}(t) = \mathrm{Tr}_E \sum_{p=1}^{D_E}\sum_{q=1}^{D_E} d^*(i,q,t)d(j,p,t)\,|j,p\rangle\langle i,q| \quad (1)$$

$$\sigma(t) = \sqrt{\sum_{i=1}^{D_S-1}\sum_{j=i+1}^{D_S} |\widetilde{\rho}_{ij}(t)|^2} \quad (2)$$

$$\delta(t) = \sqrt{\sum_{i=1}^{D_S}\left(\widetilde{\rho}_{ii}(t) - \frac{e^{-b(t)E_i^{(S)}}}{\sum_{i'=1}^{D_S} e^{-b(t)E_{i'}^{(S)}}}\right)^2} \quad (3)$$

$$e^{-\beta H} \approx \left(1 - \left\{\int_0^1 d\xi e^{-\beta\xi H_0} H_{SE} e^{\beta\xi H_0}\right\}\beta\lambda\right) e^{-\beta H_0} \quad (4)$$

$$|\Psi_0\rangle = \sum_{i=1}^{D_S}\sum_{p=1}^{D_E} d_{i,p}\,|i,p\rangle \quad (5)$$

$$\sum_{i=1}^{D_S}\sum_{p=1}^{D_E} |d_{i,p}|^2 = 1 \quad (6)$$

$$|\Psi_\beta\rangle = \frac{e^{-\beta H/2}|\Psi_0\rangle}{\langle\Psi_0|e^{-\beta H}|\Psi_0\rangle^{1/2}} \quad (7)$$

$$\begin{aligned}\mathcal{E}\left(\sigma^2\right) = {} & \frac{1}{2}e^{-2\beta(F_E(2\beta)-F_E(\beta))}\left(1-e^{-2\beta(F_S(2\beta)-F_S(\beta))}\right) \\ & -\frac{2D}{D+1}e^{-3\beta(F_E(3\beta)-F_E(\beta))} \\ & \times\left(e^{-2\beta(F_S(2\beta)-F_S(\beta))} - e^{-3\beta(F_S(3\beta)-F_S(\beta))}\right) \\ & +\frac{3D}{2(D+1)}e^{-4\beta(F_E(2\beta)-F_E(\beta))}e^{-2\beta(F_S(2\beta)-F_S(\beta))} \\ & \times\left(1-e^{-2\beta(F_S(2\beta)-F_S(\beta))}\right) \end{aligned} \quad (8)$$

$$\lim_{\beta\to 0}\mathcal{E}\left(\sigma^2\right) = \frac{D_S-1}{2(D+1)} + \mathcal{O}\left(\beta^{\in}\right) \quad (9)$$

$$\lim_{\beta\to+\infty} E(\sigma^2) = \frac{g_S-1}{2g_S g_E}\left(1-\frac{D_S D_E}{(D_S D_E+1)\,g_S g_E}\right) \quad (10)$$

$$\begin{aligned}\mathcal{E}\left(\delta^2\right) = {} & \frac{D}{D+1}e^{-2\beta(F_E(2\beta)-F_E(\beta))}\left(e^{-2\beta(F_S(2\beta)-F_S(\beta))}\right. \\ & \left.-2e^{-3\beta(F_S(3\beta)-F_S(\beta))} + e^{-4\beta(F_S(2\beta)-F_S(\beta))}\right) \\ & +e^{-2\beta(F_S(2\beta)-F_S(\beta))}\left[\left(C_S(2\beta)/(4\beta^2)\right)\right. \\ & \left.+\left(U_S(2\beta)-U_S(\beta)\right)^2\right](\Delta b)^2 \end{aligned} \quad (11)$$

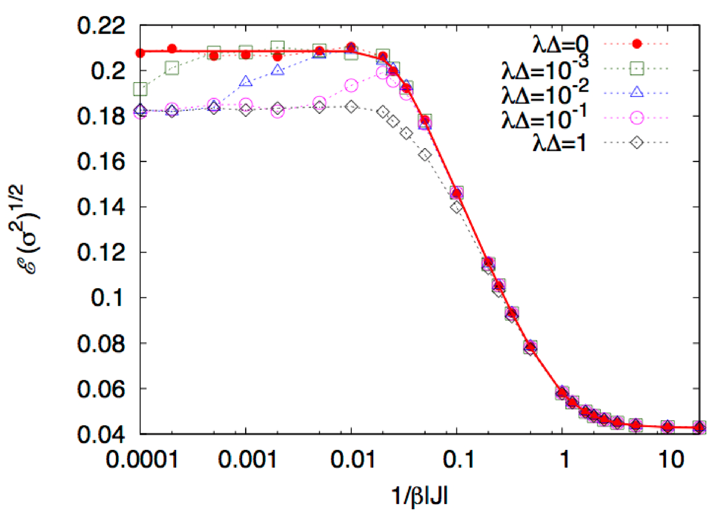

Fig. 6. $N_E=8$ ($g_E=9$), $\Omega=1$, $N_E=4$ (ferro, $J=1$, $g_S=5$). Solid red line is from Eq.(8).

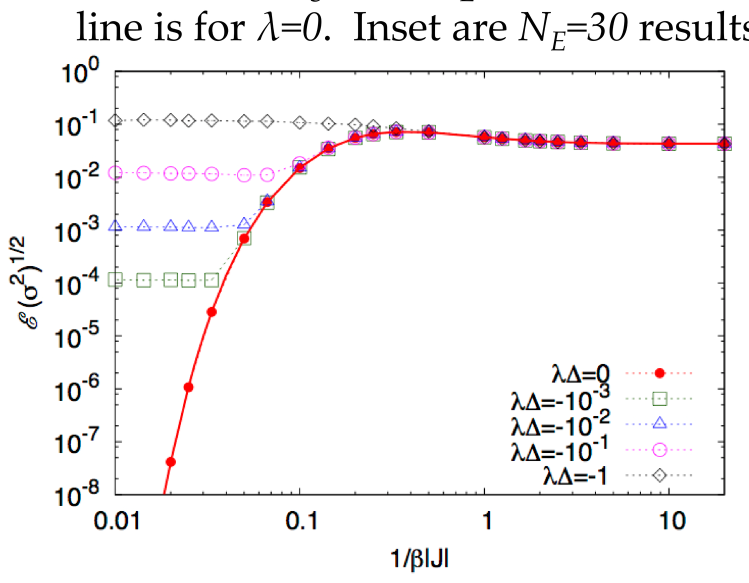

Fig. 7. $N_E=8$ ($g_E=9$), $\Omega=1$, $N_E=4$ (antiferro, $J=-1$, $g_S=1$). Solid red line is from Eq.(8).

Conclusions

We have obtained analytical results for a decoherence measure σ and thermalization measure δ, within the canonical-thermal state ensemble [1]. With minimal, reasonable assumptions we obtain Eq.(8) and Eq.(11) for σ and δ, respectively. We performed large-scale real-time and imaginary-time Schrödinger equation simulations, elucidating and testing our results. Extremely good agreement between the analytical and computational calculation results were obtained, for example in Figs. 6,7.

Reference and Acknowledgements

[1] M.A. Novotny, F. Jin, S. Yuan, S. Miyashita, H. De Raedt, and K. Michielsen, Physical Review A, vol. **92**, article 032110 [46 pages] (2016).

The authors gratefully acknowledge the computing time granted by the JARA-HPC Vergabegremium and provided on the JARA-HPC Partition part of the supercomputer JUQUEEN at Forschungszentrum Jülich. MAN is supported in part by US National Science Foundation grant DMR-1206233.